Decay-out of the yrast superdeformed band in ^{136}Nd: Towards an experimental extraction of the neutron pairing gap at large deformation

S. Perriès, A. Astier, L. Ducroux, M. Meyer, and N. Redon
Institut de Physique Nucléaire de Lyon, IN2P3/CNRS, Université C. Bernard Lyon-1, F-69622 Villeurbanne Cedex, France

C. M. Petrache, D. Bazzacco, G. Falconi, S. Lunardi, M. Lunardon, C. Rossi Alvarez, C. A. Ur, R. Venturelli, and G. Viesti
Dipartimento di Fisica and INFN, Sezione di Padova, I-35131 Padova, Italy

I. Deloncle and M. G. Porquet
Centre de Spectrométrie Nucléaire et de Spectrométrie de Masse, IN2P3/CNRS, F-91405 Orsay Campus, France

G. de Angelis, M. de Poli, C. Fahlander, E. Farnea, D. Foltescu, A. Gadea, D. R. Napoli, and Zs. Podolyàk
INFN, Laboratori Nazionali di Legnaro, I-35020 Legnaro, Italy

A. Bracco, S. Frattini, and S. Leoni
Dipartimento di Fisica and INFN, Sezione di Milano, I-20122 Milano, Italy

B. Cederwall, A. Johnson, and R. A. Wyss
Royal Institute of Technology, Physics Department Frescati, S-10405 Stockholm, Sweden
(Received 15 October 1998; published 15 November 1999)

A study of the ^{136}Nd nucleus has been performed with the EUROBALL III multidetector to establish the decay-out of the yrast superdeformed (SD) band. Three discrete linking transitions (754, 1456, and 1493 keV) have been discovered, establishing the position of the SD band at 7.03 MeV excitation energy with proposed spin and parity $17^{(-)}$ for the lowest observed SD state. Neutron pairing gap parameters for SD shapes have been extracted in Nd isotopes, using the strong-coupling model and odd-even mass difference formulas. The major conclusion of our phenomenological analysis is that the pairing correlations do subsist in the SD configurations of nuclei in the $A=130$ mass region. [S0556-2813(99)01312-6]

PACS number(s): 21.10.Re, 21.10.Tg, 23.20.Lv, 27.60.+j

I. INTRODUCTION

Since the discovery of a rotational band in the second well of ^{132}Ce [1] the study of nuclei in the $A=130$ mass region at high spin has been a fertile source of information for various phenomena concerning large deformation, like the coexistence of normal-deformed (ND) and highly deformed configurations, the role of shell gaps versus the occupation of the intruder orbitals stabilizing the large deformation and the identical bands [2–5]. In the following, for the reason of simplicity, we will use the term superdeformation (SD) in order to describe the phenomenon in the second well in this mass region, although we are aware of the fact that the difference in structure between the ND and SD states is more pronounced in other regions of the nuclear chart. The knowledge of the single-particle excitations in the second well has improved dramatically, but the lack of experimentally determined excitation energies, spins, and parities for the SD states prohibited definitive conclusions. These quantities can be reached through the observation of discrete γ transitions linking the lowest levels of the SD band to the ND ones.

The first experimental breakthrough in the knowledge of the decay-out process has been achieved in the odd ^{133,135,137}Nd nuclei of the $A=130$ mass region [6–9]. In these nuclei the observation of discrete linking transitions has been favored by the relatively high intensity of the SD bands (5–10 % of the reaction channel) as well as by the low excitation energies with respect to the yrast line in the decay-out region ($\sim$1 MeV). The SD bands in even-even Nd nuclei, being based on two quasiparticle (qp) configurations including the intruder orbital ($\nu i_{13/2}$) [10], are much weaker (about 1% of the total population of the nucleus) than in the odd-even ones, which also involve a single ($\nu i_{13/2}$) intruder orbital. The identification of discrete linking transitions in even-even nuclei is therefore as difficult as in the other regions of superdeformation ($A=80,150,190$). Such transitions have been observed only recently in ^{132,134}Nd [10,11]. The resolving power achieved by the new generation of γ-ray spectrometers, like EUROBALL III, now allows observation of transitions with intensities around 10^{-4} of the population of the final residual nucleus, making feasible the observation of linking transitions in these nuclei.

The study of the superdeformation phenomenon can also give information about pairing in states with high seniority and its variation with frequency. Indeed, the SD bands in different mass regions cover large ranges of frequencies and, if we look at the moments of inertia of the SD bands as a function of frequency, quite different behaviors are noticeable for the different regions. In the $A=190$ mass region, where the SD bands are seen down to very low spins and frequencies, the moment of inertia increases with spin due both to the gradual alignment of neutrons and protons, and to the reduction of the pairing [12–16]. However, there exists experimental signatures of the pairing persistence in the SD

configurations, like the observation of a proton blocking effect in the odd-Z ^{193}Tl nucleus [17]. On the other hand, for the $A=150$ nuclei and even more for the $A=80$ nuclei, where the SD bands are observed at very high frequencies, the rigid-body value is reached by the moment of inertia and pairing correlations have almost disappeared. In the $A=130$ mass region a large variety of SD bands were identified which show different behavior both as a function of mass number and as a function of frequency, suggesting the possible presence of pairing in the SD configurations [2]. It is, therefore, interesting to study these nuclei in order to get more precise clues on the pairing correlations. The strength of neutron (proton) pairing correlations in the second minimum of SD nuclei can be estimated by a phenomenological analysis from the knowledge of the excitation energies for a given series of isotopes (isotones). An extended series of nuclei where the SD bands were linked to ND states exists at present only in the $A=130$ mass region, where in the sequence from ^{133}Nd to ^{137}Nd, only in ^{136}Nd the SD band was not connected to low-lying states. The identification of linking transitions for the yrast SD band in ^{136}Nd will determine its excitation energy and will offer the possibility to estimate the neutron pairing gap in the second minimum by using a Taylor series expansion of the mass in powers of the nucleon number of interest.

We have undertaken the study of the decay-out of the yrast SD band in ^{136}Nd. Sections II and III contain the description of the experiment and the data analysis. Results on the decay-out are presented in Sec. IV and in Sec. V we discuss the decay-out of the yrast SD bands in the Nd series and the estimation of the pairing strength in the second well from odd-even mass differences.

II. EXPERIMENT

The experiment was performed at the Legnaro National Laboratory with the XTU Tandem accelerator. We used the same reaction and beam energy, ^{110}Pd(^{30}Si,4n) at 130 MeV, as in a previous experiment performed with the GASP array [18]. The two most intense residual nuclei populated in this reaction were ^{136}Nd and ^{137}Nd, with a ratio ^{137}Nd/^{136}Nd $\sim$20%. The target consisted of a foil of 1 mg/cm^2 of ^{110}Pd deposited on a 15 mg/cm^2 gold backing. A backed target was used to identify the transitions which depopulate the SD band. The γ-ray transitions were measured with the EUROBALL III array [19] which consisted of 239 germanium crystals. More precisely EUROBALL III consists of (i) 30 tapered germanium detectors placed on three rings at forward angles, (ii) 26 clover detectors each composed of four germanium crystals in the same cryostat at medium angles, and (iii) 15 cluster detectors formed by seven germanium capsules at backward angles. All these detectors are surrounded by BGO scintillators used for Compton suppression. The detector signals are processed through the VXI electronics which send the data to three event collectors. Finally, a processor farm builds the EUROBALL event recorded on DLT tapes. A fold condition of eight unsuppressed Ge firing in coincidence was required to start the acquisition. After Compton suppression this resulted in a total of 2.8×10^9 four- and higher-fold events collected on tape. Calibration and relative efficiencies of the array were obtained using standard sources over the range of 80–3548 keV.

III. DATA ANALYSIS

In the analysis of the events detected by the clover and cluster detectors the Compton scattering in adjacent segments has been considered. The so-called ''add-back mode'' in these composite detectors has been performed by summing the energies deposited in each involved segment. Concerning the clusters, only adjacent firing segments have been taken into account for the add-back, whereas nonadjacent ones have been treated as independent photons. We have rejected the case where more than two segments fired in one detector. The gain in efficiency (at 1.33 MeV) is then 1.29 for clovers and 1.26 for clusters when the add-back mode is used.

From previous experiments with gold backed-targets in the neighboring nuclei [7,9,18], it results that the transitions of the SD band with energies higher than $E_\gamma \simeq 800$ keV are Doppler broadened. On the contrary, the transitions de-exciting the lowest levels of the SD band appear as sharp lines in the γ-ray spectra. As the transitions which link the SD band to states of normal deformation are expected to be emitted from stopped nuclei and also to be very weak, the much better energy resolution achieved in a backed-target experiment will improve the signal-to-background ratio. In an experiment with a backed target, the Doppler correction formula reads

$$E_\gamma^{\mathrm{Detected}}(\theta) = E_\gamma^0[1+F(\tau)\beta_0\cos(\theta)], \tag{1}$$

where $E_\gamma^{\mathrm{Detected}}(\theta)$ is the energy deposited in a detector placed at an angle θ with respect to the beam axis. E_γ^0 is the center-of-mass energy of the γ ray emitted by a recoiling nucleus with a velocity $F(\tau)\beta_0$. β_0 is the initial velocity of the recoil nucleus (and has been determined to be 2.06% in our experiment) and $F(\tau)$ is the attenuation factor for each SD level. This factor reproduces the velocity decrease during the de-excitation along the SD band. Starting from the $F(\tau)$ values of ^{136}Nd and ^{137}Nd obtained from a previous GASP experiment [20], we have adjusted these factors for our experiment.

Various multiconditioned one-dimensional spectra and gated matrices have been constructed during the analysis. All one-dimensional spectra have been incremented taking into account the intensity problems first exposed in Ref. [21] and, therefore, the unphysical spikes discussed in Ref. [22]. According to Eq. (1), the SD gating conditions have been applied by using a different Doppler correction for each SD gate. Moreover the corresponding gate energy was determined for each detector angle, allowing contamination to be avoided for certain combinations of angles and energies. Usually two spectra have been obtained for each given set of gates: one spectrum with variable Doppler correction and another with $v/c=0$. The former was used to check the SD gates and the latter to search for the linking transitions.

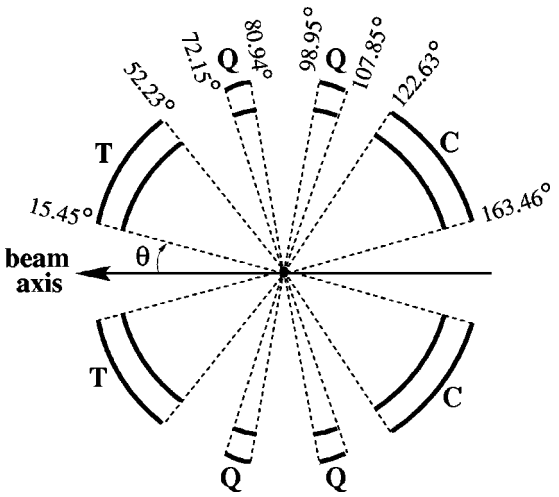

FIG. 1. Schematic angular geometry of the EUROBALL III array showing the tapered (T), clover (Q), and cluster (C) groups of detectors. Limit angles are indicated with respect to the beam axis.

Gated matrices have also been built with the same angle-dependent Doppler correction. Three kinds of matrices have been used to study the SD-ND decay path: (i) with Doppler correction on any axis to select the SD band itself, (ii) without Doppler correction to check the relationship between the linking transitions and the ND transitions, and (iii) with Doppler correction on the first axis and without it on the second one to obtain coincidence information between the SD band and the ND yrast states or SD band and the linking transitions. Directional correlations from oriented states (DCO) matrices have been built and DCO ratios have been extracted, using the EUROBALL III geometry presented in Fig. 1. By properly taking into account the angular symmetries of the correlation function $W(\theta_1,\theta_2,\Delta\phi=\phi_2-\phi_1)$ [23], we can reduce the $C^2_{239}=28\,441$ combinations of two detectors on EUROBALL III to 15 736 distinct geometries. However, the collected statistics was not enough to analyze the weak transitions of interest for all these individual geometries. The detectors of the EUROBALL III array have been separated in two sets: one with the clover (Q) detectors (located around 90° with respect to the beam axis), and the second set with all tapered (T) and cluster (C) detectors, located at forward and backward angles, respectively.

By noting $W(\text{det }1,\text{det }2)=W(\theta_1,\theta_2,\Delta\phi)$ the correlation function between the two detectors det1 and det2 at angles (θ_1,ϕ_1) and (θ_2,ϕ_2), we define then the two average correlation functions:

$$W(\mathrm{T+C,Q})=\sum_{\text{det }1\in\{\mathrm{T+C}\}}\ \sum_{\text{det }2\in\{\mathrm{Q}\}} W(\text{det }1,\text{det }2)/N_{\text{comb}},$$

$$W(\mathrm{Q,T+C})=\sum_{\text{det }1\in\{\mathrm{Q}\}}\ \sum_{\text{det }2\in\{\mathrm{T+C}\}} W(\text{det }1,\text{det }2)/N_{\text{comb}}, \tag{2}$$

where $N_{\text{comb}}=14\,040$ is the number of distinct pairs (T+C,Q), i.e., the number of tapered (30) and cluster segments

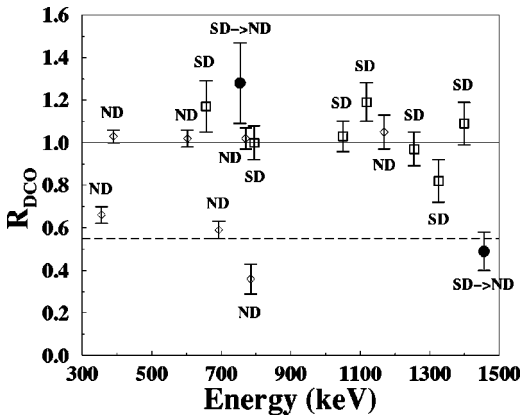

FIG. 2. Experimental DCO ratios for ND, SD, and linking SD-ND transitions of ^{136}Nd. The solid and dashed lines correspond to the theoretical DCO values of the stretched quadrupole-quadrupole and dipole-quadrupole sequences, respectively.

$(7\times15=105)$, multiplied by the number of clover crystals $(4\times26=104)$. We can, therefore, define a ''generalized'' DCO ratio by

$$R_{\text{DCO}}=\frac{W(\mathrm{T+C,Q})}{W(\mathrm{Q,T+C})}. \tag{3}$$

The theoretical DCO ratio derived for this geometry has been calculated for a cascade $I_1\rightarrow I_2\rightarrow I_3$, starting from a completely aligned state with $I_1=21$. For each pair (T+C,Q), the corresponding value lies in the interval [0.41,0.80] for a stretched dipole-quadrupole sequence, depending on the considered detector pair. For $I_1>10$ this DCO ratio is roughly independent of spins. The average value is $R_{\text{DCO}}=0.55$ for a stretched dipole-quadrupole sequence. It is, therefore, easily distinguishable from any stretched quadrupole-quadrupole sequence which has a DCO ratio of 1.00. For illustration we present in Fig. 2 the extracted DCO ratios of several ND, SD, and SD-ND linking transitions. The results are also listed in Table I. Known dipole and quadrupole multipolarities [24] are clearly confirmed by our measurements and we have been able to determine the multipolarity order of two SD-ND linking transitions, as it will be discussed below.

IV. RESULTS

The decay-out spectrum of the SD band of ^{137}Nd, a by-product of this experiment, is shown in Fig. 3. The same discrete linking transitions observed previously in a GASP experiment [9] are seen here with better statistics, demonstrating the power of the EUROBALL III array.

Spectra with and without Doppler correction obtained for ^{136}Nd are presented in Figs. 4 and 5. We confirm all SD transitions observed in the GASP experiment [18], and up to the 1644 keV transition observed in the GAMMASPHERE experiment [25]. The 1733 keV transition is at the observation limit of our experiment and we have not seen the last transition with energy of 1815 keV tentatively proposed in Ref. [25]. In Fig. 4(a) γ rays with energies higher than 717 keV are Doppler corrected, including the linking transitions

TABLE I. Experimental intensities and DCO ratios (see text for explanation) for ND, SD, and SD-ND linking transitions in ^{136}Nd. Gates on $E2$ transitions have been used to extract the DCO value for each transition. The DCO ratio of the transitions marked by an asterisk are displayed in Fig. 2. Intensities are normalized at 100% for the 857 keV SD transition and correspond to the decay-out of the SD band as displayed in Fig. 8.

E_γ (keV)	Intensity (%)	DCO ratio	Assignation
ND transitions			
355.4(2)*	24(5)	0.66(4)	$10^+ \rightarrow 9^-$
373.7(2)*	100(8)	1.01(3)	$2^+ \rightarrow 0^+$
390.1(2)	88(8)	1.03(4)	$12^+ \rightarrow 10^+$
501.2(2)	20(4)	0.96(5)	$9^- \rightarrow 7^-$
552.1(2)	6(2)	1.10(5)	$12^+ \rightarrow 10^+$
602.7(2)*	100(9)	1.02(4)	$4^+ \rightarrow 2^+$
661.3(3)	70(9)		$14^+ \rightarrow 12^+$
663.7(3)	68(9)		$10^+ \rightarrow 8^+$
678.4(4)	15(4)		$15^+ \rightarrow 13^+$
693.5(2)*	23(4)	0.59(4)	$7^- \rightarrow 6^+$
711.8(3)	6(2)		$14^+ \rightarrow 12^+$
714.5(2)	11(3)	0.98(4)	$16^+ \rightarrow 14^+$
750.4(2)	6(2)	0.30(6)	$17^+ \rightarrow 16^+$
768.7(6)	13(8)		$13^+ \rightarrow 12^+$
770.4(2)*	100(10)	1.02(5)	$6^+ \rightarrow 4^+$
784.9(2)*	11(4)	0.36(7)	$15^+ \rightarrow 14^+$
809.9(3)	7(3)		$17^+ \rightarrow 15^+$
844.3(3)	5(2)		$16^+ \rightarrow 14^+$
844.7(2)	45(7)	1.01(4)	$16^+ \rightarrow 14^+$
886.0(2)	76(8)	1.04(5)	$8^+ \rightarrow 6^+$
894.6(4)	4(2)		$18^+ \rightarrow 16^+$
901.6(2)	9(3)	1.01(7)	$18^+ \rightarrow 16^+$
999.7(2)	20(4)	0.91(6)	$18^+ \rightarrow 16^+$
1135.7(3)	6(3)	0.95(5)	$10^+ \rightarrow 8^+$
1169.2(3)	9(3)	1.05(8)	$14^+ \rightarrow 12^+$
1222.6(4)*	11(4)	1.10(7)	$16^+ \rightarrow 14^+$
1279.7(9)	5(3)	0.92(4)	$18^+ \rightarrow 16^+$
SD transitions			
656.6(3)*	14(4)	1.17(12)	$19^{(-)} \rightarrow 17^{(-)}$
716.7(7)	52(15)		$21^{(-)} \rightarrow 19^{(-)}$
795.0(5)*	95(14)	1.00(8)	$23^{(-)} \rightarrow 21^{(-)}$
857.9(5)	100(13)		$25^{(-)} \rightarrow 23^{(-)}$
918.4(6)	99(14)		$27^{(-)} \rightarrow 25^{(-)}$
983.7(3)	101(13)		$29^{(-)} \rightarrow 27^{(-)}$
1050.1(4)*	103(13)	1.03(7)	$31^{(-)} \rightarrow 29^{(-)}$
1117.5(4)*	95(12)	1.19(9)	$33^{(-)} \rightarrow 31^{(-)}$
1186.2(4)	54(9)		$35^{(-)} \rightarrow 33^{(-)}$
1254.9(4)*	39(7)	0.97(8)	$37^{(-)} \rightarrow 35^{(-)}$
1325.3(5)*	23(4)	0.82(10)	$39^{(-)} \rightarrow 37^{(-)}$
1398.9(4)*	20(4)	1.09(10)	$41^{(-)} \rightarrow 39^{(-)}$
1476.6(5)	12(3)		$43^{(-)} \rightarrow 41^{(-)}$
1559.1(5)	6(2)		$45^{(-)} \rightarrow 43^{(-)}$
1644.4(7)	3(2)		$47^{(-)} \rightarrow 45^{(-)}$
SD→ND transitions			
754.2(3)*	15(4)	1.28(19)	$21^{(-)} \rightarrow 19^{(-)}$
1456(1)*	11(4)	0.49(9)	$19^{(-)} \rightarrow 18^+$
1493(1)	6(3)		$19^{(-)} \rightarrow 18^+$

which should not be. In the uncorrected spectrum shown in Fig. 4(b) the SD transitions appear as broad bumps while all ND transitions look like sharp lines. This is the clear signature that the SD γ rays have been emitted during the recoiling time of the nucleus, while ND transitions have been emitted by the stopped nucleus. In this last spectrum, linking transitions, if they exist, should be sharp. The high-energy part of the uncorrected spectrum given in Fig. 5 provides, among the Doppler broadened SD transitions, three candidates for the linking transitions, namely the 1456, 1603, and 1743 keV lines. In order to establish the position of these candidates in a decay-out level scheme, we have studied the coincidence relationships between SD and ND transitions.

The spectra obtained by double-gating on the 390 keV $12^+ \rightarrow 10^+$ ND transition and one among two of the lowest transitions of the SD band—either 717–795 keV [Fig. 6(a)], or 795–857 keV [Fig. 6(b)]—show a new sharp line at 1493 keV. This transition cannot be seen in Fig. 5, because it is unresolved in the 1477 keV SD bump. The comparison between the spectra 6(a) and 6(b) shows that the 1456 keV line is weaker in the first one, while the 1493 keV intensity is unchanged. This means that the 1493 keV transition is in coincidence with the 717 keV SD transition whereas the 1456 keV one is not. Another new transition of 754 keV is in coincidence with SD band members, but not with the 717 keV SD transition. A clear coincidence relationship between the 1456 keV line and the 754 keV transition has been also observed, as demonstrated by Figs. 7(a) and 7(b).

This analysis shows that the linking transitions reach the

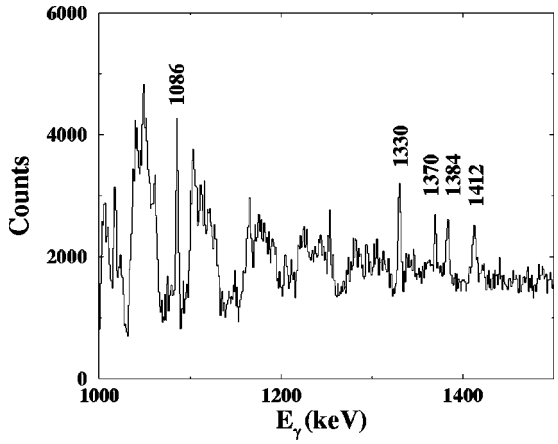

FIG. 3. Double-gated background subtracted spectrum of the ^{137}Nd SD band, obtained without Doppler correction. The broad structures correspond to the SD transitions widened by the Doppler effect. The energies of the linking transitions between the SD band and the ND states are indicated.

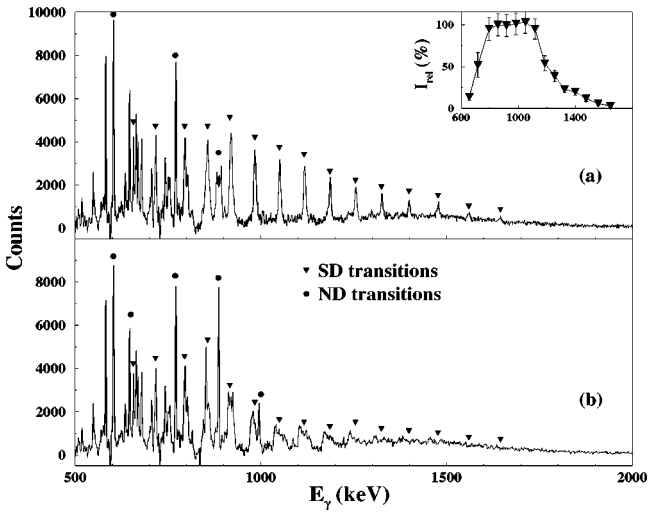

FIG. 4. Double-gated background subtracted spectra of the ^{136}Nd yrast SD band. SD transitions (657, 717, 795, 857, 918, 984, 1050, 1117, 1186, 1255, 1325, 1399, 1477, 1559, and 1644 keV) are indicated by down triangles and ND transitions by circles. The upper spectrum (a) has been Doppler corrected, while the lower one (b) has not been corrected. The relative intensity profile of the SD band is also plotted in the inset.

ND levels at the 18^+ level de-excited by the 1000 keV γ line. The two parallel γ-ray cascades 1456–754 keV and 1493–717 keV establish an energy difference of 2210 keV between the third low-lying state of the SD band at spin $21^{(-)}$ and the 18^+ of band 3. Figure 8 displays the level scheme associated with the decay-out of the yrast SD band in ^{136}Nd. The DCO ratios of the linking transitions (see results in Table I and Fig. 2) show that the 1456 keV transition is dipolar ($\Delta I=1$), while the 754 keV transition is quadrupolar ($\Delta I=2$). If we assume a negative parity for the SD band (as suggested also in ^{132,134}Nd [10,11]), the decay-out proceeds via $E2$ and $E1$ transitions. Therefore, the lowest observed state of the SD band at an excitation energy of 7028 keV is tentatively proposed to have spin and parity $17^{(-)}$. The 1603 and 1743 keV transitions mentioned above are involved in

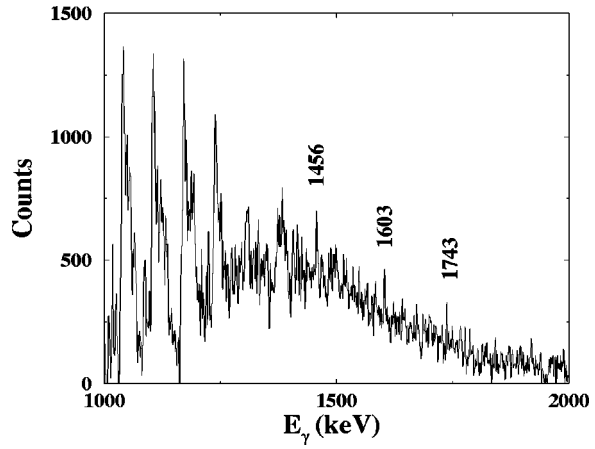

FIG. 5. High-energy part of Fig. 4(b). Broad peaks are the SD transitions widened by the Doppler effect. The energies of the linking transition candidates are indicated.

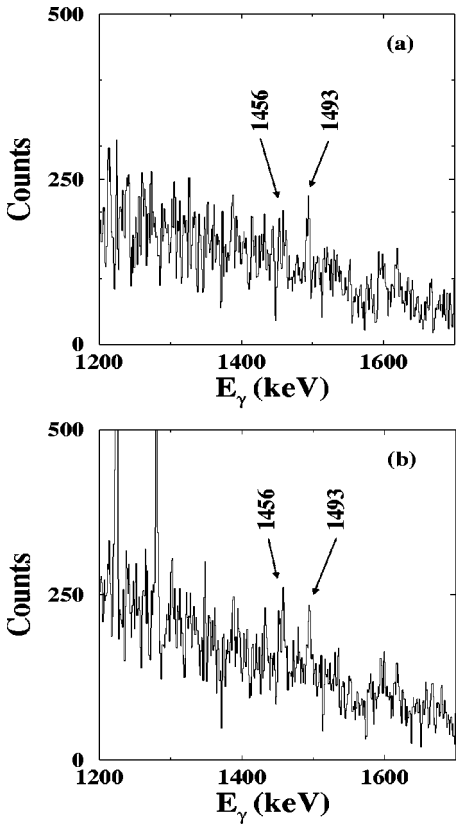

FIG. 6. Spectra in coincidence with the 390 keV ND transition and with one among two of the lowest SD transitions, namely 717 keV or 795 keV (a), and 795 keV or 857 keV (b).

the decay scheme of the SD band but we could not establish any clear coincidence relationship with individual transitions and, therefore, we could not place them in the level scheme.

In Fig. 8 are indicated the observed linking transitions and also the intensities of the decay-out flow, the reference being taken for the 857 keV transition (100%). The intensities of all transitions involved in the decay-out of the SD band are listed in Table I.

The observed discrete linking transitions collect about 20% of the SD decay-out intensity via the two transitions of 754 and 1493 keV. As detailed previously, clear coincidence relationships have been observed, establishing unambiguously the position of the three linking transitions 754, 1456, and 1493 keV. Concerning the order of the 754–1456 keV sequence, where the 754 keV transition is more intense than the 1456 keV transition (see Table I), we have chosen the order displayed in Fig. 8 because it gives a non-yrast intermediate level in agreement with its weak population. It is worth noting that the same argument has been used in [10] for the decay-out of the yrast SD band of ^{134}Nd which presents a very similar pattern to the ^{136}Nd one. The $19^{(-)}$ level populated by the 754 keV transition decays also by means of other unseen transitions with relative intensity of around 4%.

The extracted intensities provide also information on the fragmentation of the decay-out. One can see that the decay-out flow of the SD band is distributed towards the three structures called bands 3, 4, and 5 in Refs. [18,24], with

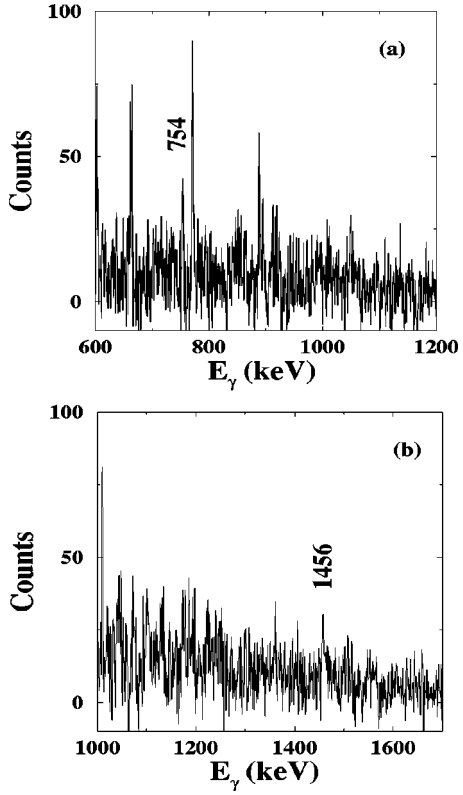

FIG. 7. Spectra in coincidence with two SD transitions plus the 1456 keV linking transition (a), and with two SD transitions plus the 754 keV transition (b).

$\sim$30% each. A fourth band (labeled band 7) receives only about 4% of the decay-out. Note that these bands are expected to have triaxial shapes and are assumed to involve one pair of aligned $h_{11/2}$ neutrons (at $\gamma=-90°$) or protons (at $\gamma=+30°$) [18]. The full SD intensity is completely recovered at spin $15-16\hbar$.

V. DISCUSSION

One of the most challenging questions concerning the superdeformation phenomenon is the decay-out of the SD bands and the understanding of their main features: decay through discrete γ rays to low-lying ND states or through a continuum of states, properties of the preferentially populated ND states, pairing effects in the SD bands. The Nd series represent a very appropriate laboratory for such studies because the evolution of the decay out with the neutron number N can now be analyzed, including the results of the present paper, in six Nd isotopes with neutron number from $N=72$ to $N=77$, namely, $^{132-137}$Nd [6–11].

A. SD decay-out in the Nd isotopes

The SD magic numbers in the $A=130$ mass region are $Z=58$ and $N=72$, which correspond to the ^{130}Ce nucleus, stabilizing elongated shapes with an axis ratio 3/2 and a β_2 value around 0.35–0.4. A sizable proton gap exists also for $Z=60$ at somewhat smaller deformation ($\beta_2\sim0.30$), which associated to the $N=72$ neutron gap, gives ^{132}Nd as the doubly closed SD magic nucleus at zero frequency. The effect of the deformation takes its origin from the occupation of the down-sloping $i_{13/2}$ intruder orbital. The neutron orbitals as function of the axial quadrupole deformation obtained in standard Nilsson calculations is presented in Fig. 9. The valence SD neutron orbitals for ^{136}Nd at $\beta_2\sim0.3$ are $h_{11/2}$ [523]7/2, $h_{9/2}$ [541]1/2, $g_{7/2}$ [402]5/2, and $g_{7/2}$ [404]7/2 below the Fermi level, and $h_{11/2}$ [514]9/2, $f_{7/2}$ [530]1/2, $h_{9/2}$ [532]3/2, and $i_{13/2}$ [660]1/2 above the Fermi level. For large deformations a sizable gap appears clearly for $N=72$ (^{130}Ce and ^{132}Nd) around $\beta_2=0.35-0.40$, whereas smaller gaps remain for $N=74$ and $N=76$ around $\beta_2=0.30-0.33$ and $\beta_2=0.28-0.30$, respectively.

The axial deformation is predicted to be slightly larger in ^{132}Nd than in ^{134}Nd or even in ^{136}Nd. We have to notice that these shell gaps are predicted in all static mean-field calcu-

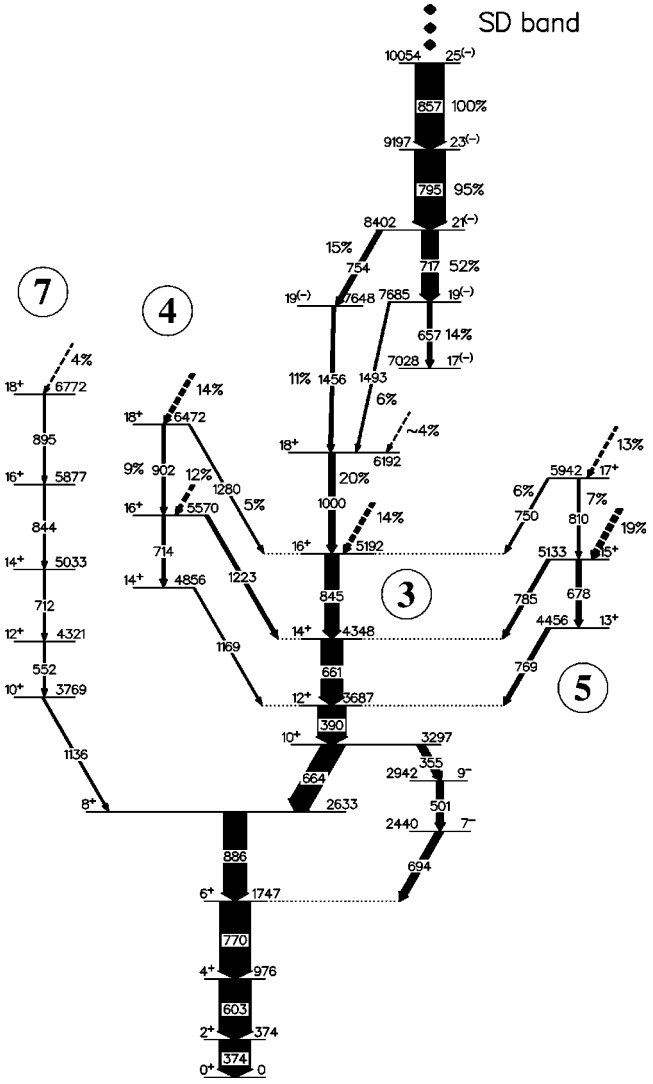

FIG. 8. Level scheme associated with the decay-out of the ^{136}Nd yrast SD band. Displayed intensities are normalized at 100% for the 857 keV SD transition. Band labels 3, 4, 5, and 7 are the same used in Refs. [18,24]. Dashed arrows indicate the intensity received by the ND levels directly fed by the SD decay-out. The widths of the arrows are indicative of the intensities listed in Table I.

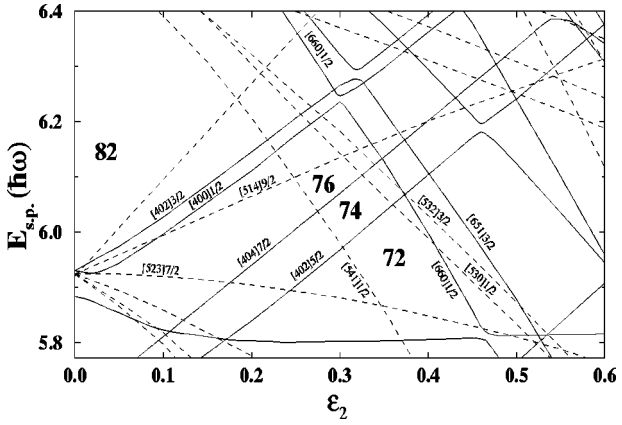

FIG. 9. Valence neutron orbitals as function of axial quadrupole deformation obtained in standard Nilsson calculations, from [26].

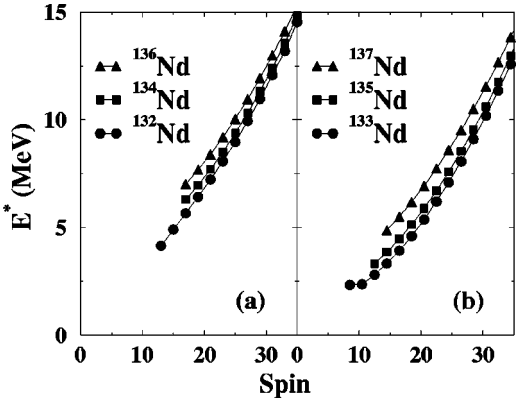

FIG. 10. Comparison of the SD states excitation energies versus the spin, for even-even (a) and odd-even Nd isotopes (b).

lations (Woods-Saxon [4], Hartree-Fock+BCS with SIII or SkM* parametrizations of the effective force [27]). The fast rotation alters these static shell effects, leading to a gap for $N=73$ at a frequency of about 0.5 MeV. When the nucleus rotates, the $i_{13/2}$ [660]1/2 orbital splits into two signature partners, which we will denote as 6_1 and 6_2. In the second minimum of the Nd isotopic series the intruder orbital [660]1/2 is occupied, and the SD bands are built on one-quasiparticle (1-qp) configurations in odd-even isotopes and 2-qp configurations in even-even isotopes. For ^{132}Nd the yrast SD band is built on the 2-qp configuration [660]1/2 $\otimes$[541]1/2 at low spin and [660]1/2$\otimes$[523]7/2 at higher spins. For the ^{134}Nd and ^{136}Nd yrast SD bands, the 2qp configurations [660]1/2$\otimes$[541]1/2 or [660]1/2$\otimes$[530]1/2 have been proposed [10,18].

Total routhian surface (TRS) calculations have been performed in this mass region [4–6,18], that suggest the SD bands in the even-even Nd isotopes are built upon 2-qp configurations. This is in contrast to the structure of the SD band in ^{132}Ce, which involves a pair of $\nu i_{13/2}$. The moment of inertia of the bands with such a configuration exhibits a pronounced band-crossing associated with the alignment of the $i_{13/2}$ orbital [4]. The absence of that band-crossing in all of the Nd isotopes strongly supports the $6_1\otimes h_{9/2}/f_{7/2}$ configuration. The difference between the Nd and Ce SD nuclei can partly be accounted for by the more deformed $Z=58$ gap. A similar situation can be found in the $A=150$ region, where, e.g., the lowest SD bands in ^{148}Gd is interpreted in terms of a 2-qp configuration [28,29].

We will now shortly discuss the different properties of the decay-out in the Nd series, like the intensities of the discrete linking transitions, the excitation energy of the SD bands, and the nature of the decay-out mechanism.

The most striking feature of the discrete linking transitions discovered in the Nd series is that the total intensity of the observed discrete decay-out transitions decreases with increasing mass number, with a stronger absolute value for odd-even isotopes: 100% for ^{133}Nd, 65% for ^{135}Nd, 30% for ^{137}Nd and 100% for ^{132}Nd, 50% for ^{134}Nd, 20% for ^{136}Nd. One has to remember that the absolute intensity of the SD bands is 5–10 % of the reaction channel for odd-even isotopes and 1% for even-even ones. This behavior can be understood by an increase of the excitation energy with A, as can be seen in Fig. 10, which presents the excitation energy of the SD states as a function of spin in the Nd isotopes, including the results of this work [7–11]. A simple explanation of this pattern can be given in terms of the shell structure at $N=72,73$ and the evolution of the shape of the ND structures in the Nd isotopes. As is well known from other regions of the nuclear chart and discussed in detail in Ref. [30], the quadrupole deformation of the heavy Nd isotopes is decreasing with increasing N, and becomes spherical at the $N=82$ shell closure. More deformed structures, involving the occupation of the 6_1 orbital, are therefore becoming more costly in energy with respect to the ND ground state, despite the increase in N. Moreover, the excitation energy of the SD bands is systematically higher in even-even isotopes than in the odd-even ones, a fact which can be related to the nature of the SD configuration, which is 2 qp in even-even and 1 qp in odd-even nuclei. The cases of ^{132,133}Nd are particular because the SD bands seem to survive at extremely low spins, reflecting their strong mixing with the ND bands and, in fact, the last SD states are probably mixtures of low and high deformations.

The nature of the decay-out mechanism involved in the $A=130$ mass region, namely in the Nd series, has been discussed in Ref. [2] and very recently in Ref. [31], where new experimental information on the decay-out of two SD bands in ^{132,134}Nd was reported. The observed $E2$ linking transitions of the SD bands with assigned positive parity were explained by the crossing of the SD bands with observed nonyrast bands of normal deformation; in this case large interaction matrix elements (V$\sim$30 keV) and large mixing amplitudes (20–30 %) between the interacting SD and ND bands were deduced. These new results clearly show that the barrier between the SD and ND minima disappears at low spin. The decay-out in the $A=130$ mass region differs thus strongly from that of the $A=190$ mass region as observed in ^{194}Hg and ^{194}Pb isotopes [32–36]. In these nuclei, the SD de-excitation is dominated by a statistical component [37] and the discrete high-energy lines ($\sim$3 MeV) contribute to only a few percent of the decay spectrum, whereas in the Nd

isotopes the decay-out is dominated by discrete lines with much lower energies (<1.5 MeV) and reach 100% of the band intensity for the lightest isotopes.

B. Pairing correlations in the superdeformed configurations

The knowledge of the SD absolute excitation energy for an extended series of Nd isotopes, enables the pairing gap to be estimated in the second minimum. Indeed, it is well known for ND matter that an estimation of the neutron pairing gap Δ_n (or proton pairing gap Δ_p) can be obtained from the odd-even mass differences using a first-order Taylor expansion [see in the Appendix, Eq. (A5)] [38–40]. The experimental neutron pairing gap takes the following expression:

$$\Delta_n = \frac{(-)^N}{2}[M(N+1) - 2M(N) + M(N-1)]. \quad (4)$$

In fact, it has been shown experimentally that Δ_n is smaller for nuclei with odd neutron numbers N than those with even N numbers. For $N=Z$ nuclei this odd-even staggering has been related to the pairing and also to the deformation of the mean field [41]. In order to smooth possible local discontinuities a third-order Taylor expansion with five points can be similarly derived.

A similar procedure to estimate the neutron pairing gap can be applied to the SD nuclei, for instance to the ^{192,193,194}Pb nuclei, where candidate and definite linking transitions have been proposed [35,42,43]. In this case, for even-even nuclei the ground state in the SD minimum is the 0 qp vacuum, labeled 0 qp_{SD}, while the ground state of odd nuclei is a 1 qp_{SD} state. The expression for the neutron pairing strength derived with the three point formula is then

$$\Delta_n^{\mathrm{SD}(0\ \mathrm{qp}-1\mathrm{qp})} = \frac{(-)^N}{2}[M^{\mathrm{SD}}(N+1) - 2M^{\mathrm{SD}}(N) + M^{\mathrm{SD}}(N-1)], \quad (5)$$

where M^{SD} is the nuclear mass in the ground-state SD minimum. The same is valid for the proton pairing gap, which can be estimated from the series ^{192}Hg, ^{193}Tl, ^{194}Pb. The extraction of Δ_n and Δ_p for the $A=190$ SD mass region will be discussed in a separate paper [44].

The situation for the SD Nd isotopes is different. As commonly adopted and discussed above, the yrast SD bands in even-N isotopes are based on a 2 qp_{SD} state, and in odd-N ones on a 1 qp_{SD} state. Indeed, as shown by potential energy curves versus deformation, obtained in constrained Hartree-Fock+BCS calculations [27], there is no well-defined SD minimum corresponding to 0 qp. However, a SD minimum is stabilized by the addition of two (one) quasiparticles including the [660]1/2 orbital for even (odd) nuclei. For such a case of SD nuclei involving 2 qp and 1 qp in even and odd isotopes, respectively, it is possible to derive the following formula from Eq. (A8):

$$\Delta_n^{\mathrm{SD}(2\mathrm{qp}-1\mathrm{qp})} = \frac{(-)^{N+1}}{2}[M^{\mathrm{SD}}(N+1) - 2M^{\mathrm{SD}}(N) + M^{\mathrm{SD}}(N-1)]. \quad (6)$$

Up to now this formula has no direct application in the $A=130$ SD matter because SD bandhead excitation energies are not known and we have to estimate the rotational contribution between the SD ground state and the lowest experimentally observed SD states. Nevertheless, for the Nd series it is possible to correlate under different assumptions the odd-even mass differences to the pairing gap. In the strong-coupling scheme limit of the particle-plus-rotor model [40], for axial symmetry the excitation energy of a state at spin I is the sum of the collective rotational energy, $\hbar^2/2\mathcal{J}[I(I+1) - K^2]$, where $\mathcal{J}$ is the moment of inertia and K the projection of I on the symmetry axis, and of the intrinsic energy, which is the sum of the individual quasiparticle energies. In this limit we have neglected the Coriolis interaction. For $K=1/2$ orbitals we also neglect, when applying the mass formula, the difference of the contributions coming from the decoupling factor terms in the odd-N (1 qp) and even-N (2 qp) nuclei. In the case of two quasiparticles, the intrinsic energy is $E_{K_1}+E_{K_2}$ and $K=|K_1 \pm K_2|$. At a given spin I the mass of an even SD nucleus is given by

$$M_I^{\mathrm{SD}}(2\ \mathrm{qp}) = M_{0^+}^{\mathrm{SD}}(0\ \mathrm{qp}) + \frac{\hbar^2}{2\mathcal{J}}[I(I+1) - K^2] + E_{K_1} + E_{K_2}. \quad (7)$$

For the odd-N SD nucleus with 1 qp in the orbital K_1 the equation is

$$M_I^{\mathrm{SD}}(1\mathrm{qp}) = M_{gs}^{\mathrm{SD}}(1\mathrm{qp}) + \frac{\hbar^2}{2\mathcal{J}}[I(I+1) - {K_1}^2]. \quad (8)$$

If we assume that the rotational contribution is the same for three Nd isotopes, that is to say (i) a similar deformation leading to the same moment of inertia $\mathcal{J}$ and (ii) K^2 and K_1^2 negligible in comparison to $(\hbar^2/2\mathcal{J})I(I+1)$, it is justified to suppose that the same formulas remain valid at a given spin I:

$$\Delta_n^{\mathrm{SD}(2\ \mathrm{qp}-1\mathrm{qp})}(I) = \frac{(-)^{N+1}}{2}[M_I^{\mathrm{SD}}(N+1) - 2M_I^{\mathrm{SD}}(N) + M_I^{\mathrm{SD}}(N-1)], \quad (9)$$

choosing for each nucleus SD states at the same spin I approximately.

The application of the strong-coupling scheme is valid only for moderate spin values up to $\sim 30\hbar$ and for large deformations. In the Nd series it is therefore reasonable to apply this simple model instead of the cranking model.

The $\mathcal{J}^{(2)}$ dynamical moments of inertia have quite similar values in the spin range 20–40 $\hbar$, compatible with the similar deformation assumption. The SD bands in odd-even Nd nuclei are based on the [660]1/2 orbital ($K_1=1/2$) and those in the even Nd are based on a 2-qp state, one being the same [660]1/2 intruder orbital ($K_1=1/2$) and the other having the

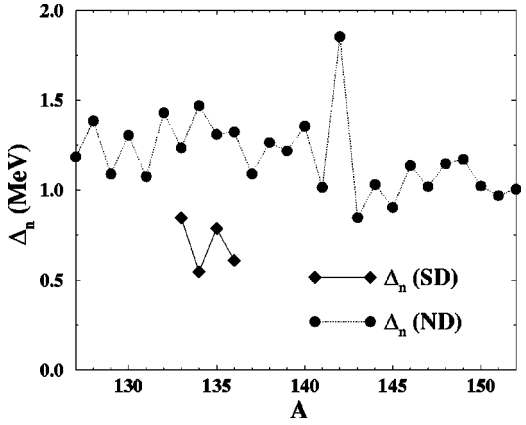

FIG. 11. Experimental neutron pairing gaps for $^{133-136}$Nd at SD shapes and for $^{127-152}$Nd in their ND ground states. SD points correspond to the mean values of Δ_n, extracted within the spin range of the SD bands.

projection $K_2=1/2$ (from the [541]1/2 or the [530]1/2 orbital). So for spins around 20 the contributions of ${K_1}^2$ and ${K_2}^2$ are really negligible.

The complete results for $^{133-136}$Nd are shown in Fig. 11 for ND and SD shapes. The most striking feature of our results is that the pairing gap parameter for the SD shapes is reduced by a factor of 2 with respect to the ND value ($\Delta_n^{\mathrm{SD}} \sim 0.7$ MeV), indicating that pairing correlations still exist in the SD matter. For 2-qp states (as discussed by Jain *et al.* [45]) a reduction by about 20% is expected due to the blocking effect, but here the quenching is stronger. However, because of the crude assumptions, our extraction is very rough and the estimated values have maximum errors of about 50%, half of it being due to the experimental ND mass values used. We have also to note that the gap values remain rather constant with increasing spin, having a reversed odd-even staggering due to the use of the 2 qp–1 qp formula for SD nuclei instead of the 0 qp–1 qp formula for ND nuclei. The results of the present phenomenological analysis are in perfect agreement with our extended TRS calculations, which yield the following values of the neutron pairing gap for the series of Nd isotopes (in MeV): 0.65 (^{132}Nd), 0.86 (^{133}Nd), 0.67 (^{134}Nd), 0.78 (^{135}Nd), 0.75 (^{136}Nd), 0.88 (^{137}Nd), at the frequency $\hbar\omega=0.25$ MeV. We can notice that both the absolute values of the pairing gap and the odd-even effect leading to lower values for even-even isotopes are well reproduced. The experimental results are also in agreement with the cranked Hartree-Fock-Bogoliubov (HFB) calculations of Ref. [46], which predicted that the neutron pairing gap remains finite even at spin 60 in the ^{136}Nd SD band.

VI. CONCLUSION

We have observed for the first time, by using the EUROBALL III array, discrete γ-ray linking transitions deexciting the SD band in ^{136}Nd, accounting for 20% of the decay-out flux. The position of the SD band in the level scheme has been established. From DCO analysis, we propose that the lowest observed SD state, located at the excitation energy of 7.03 MeV, has a spin-parity $17^{(-)}$. The total decay-out flow is collected at spin $15–16\hbar$ on mainly four ND structures. We have also estimated the neutron pairing gap in the SD matter, using the strong-coupling model with restrictive hypothesis, which led to the conclusion that pairing correlations still exist in the SD bands of the $A=130$ mass region. This result is confirmed by extended TRS calculations including pairing. Microscopic self-consistent cranked Hartree-Fock-Bogoliubov calculations should be performed in order to confirm and quantify the quenching of the neutron pairing gap in this region.

ACKNOWLEDGMENTS

We are greatly indebted to the EUROBALL III acquisition staff members for their continuous support during the experiment. We also thank J. Sharpey-Schafer and J. Meyer for illuminating discussions.

APPENDIX

In an isotopic series of nuclei characterized by Z let us consider the three isotopes with neutron numbers $N-1$, N, and $N+1$, with N even. The total binding energy $B^{1\mathrm{qp}}(N+1)$, defined negative, of the nucleus $N+1$ in its ground state (which corresponds to one quasiparticle) is related to the binding energy $B^{0\ \mathrm{qp}}(N)$ of the nucleus N in its ground state (i.e., with zero quasiparticle), the Fermi energy λ and the lowest quasiparticle energy of the odd neutron E_{K_1} by

$$B^{1\mathrm{qp}}(N+1)=B^{0\ \mathrm{qp}}(N)+\lambda+E_{K_1}. \tag{A1}$$

In the BCS formalism E_{K_1} is related to the single-particle energy e_{K_1} and the neutron gap parameter Δ by the relation

$$E_{K_1}=\sqrt{(e_{K_1}-\lambda)^2+\Delta^2}. \tag{A2}$$

The total binding energy $B^{1\mathrm{qp}}(N-1)$ of the nucleus $N-1$ is expressed as

$$B^{1\mathrm{qp}}(N-1)=B^{0\ \mathrm{qp}}(N)-\lambda+E_{K_1}. \tag{A3}$$

Therefore, the gap parameter Δ characterizing the pairing term can be derived from the usual odd-even mass differences as [38,39]

$$\begin{aligned}&\frac{1}{2}[M(N+1)-2M(N)+M(N-1)]\\&=\frac{1}{2}[B^{1\mathrm{qp}}(N+1)-2B^{0\ \mathrm{qp}}(N)+B^{1\ \mathrm{qp}}(N-1)]\\&=E_{K_1}\simeq+\Delta.\end{aligned} \tag{A4}$$

The same formula with an opposite sign can be derived for odd N [40]. We can, therefore, write the generalized formula for the neutron pairing gap:

$$\Delta^{(0\ \mathrm{qp}-1\ \mathrm{qp})}=\frac{(-)^N}{2}[M(N+1)-2M(N)+M(N-1)]. \tag{A5}$$

If we consider now the nucleus N in an excited state corresponding to a two-quasiparticle state of energy $(E_{K_1}+E_{K_2})$, one of the two quasiparticles being that of the odd neutron in the $N+1$ and $N-1$ nuclei, the total binding energy for the nucleus N is the sum:

$$B^{2\ \mathrm{qp}}(N)=B^{0\ \mathrm{qp}}(N)+E_{K_1}+E_{K_2}. \tag{A6}$$

The odd-even mass differences can then consequently be related approximately to an average gap parameter as

$$\begin{aligned}\frac{1}{2}[M^{1\ \mathrm{qp}}(N+1)-2M^{2\ \mathrm{qp}}(N)+M^{1\ \mathrm{qp}}(N-1)]&\\ =\frac{1}{2}[B^{1\mathrm{qp}}(N+1)-2B^{2\ \mathrm{qp}}(N)+B^{1\ \mathrm{qp}}(N-1)]&\\ \simeq -E_{K_2}\simeq-\Delta.&\end{aligned} \tag{A7}$$

And similarly, extending to any N value the neutron gap parameter is then

$$\begin{aligned}\Delta^{(2\ \mathrm{qp}-1\ \mathrm{qp})}=\frac{(-)^{N+1}}{2}[M^{1\ \mathrm{qp}}(N+1)-2M^{2\ \mathrm{qp}}(N)&\\ +M^{1\ \mathrm{qp}}(N-1)].&\end{aligned} \tag{A8}$$

However, because two quasiparticles K_1 and K_2 are blocked, a reduction of the pairing gap is expected.

[1] P. J. Nolan, A. J. Kirwan, D. J. G. Love, A. H. Nelson, D. J. Unwin, and P. J. Twin, J. Phys. G **11**, 217 (1985).
[2] C. M. Petrache, Z. Phys. A **358**, 225 (1997), and references therein.
[3] A. T. Semple *et al.*, J. Phys. G **24**, 1125 (1998), and references therein.
[4] R. Wyss, J. Nyberg, A. Johsonn, R. Bengtsson, and W. Nazarewicz, Phys. Lett. B **215**, 211 (1988).
[5] C. M. Petrache *et al.*, Phys. Lett. B **387**, 31 (1996).
[6] D. Bazzacco *et al.*, Phys. Lett. B **309**, 235 (1993).
[7] D. Bazzacco *et al.*, Phys. Rev. C **49**, R2281 (1994).
[8] M. Deleplanque *et al.*, Phys. Rev. C **52**, R2302 (1995).
[9] S. Lunardi, R. Venturelli, D. Bazzacco, C. M. Petrache, C. Rossi-Alvarez, G. de Angelis, G. Vedovato, D. Bucurescu, and C. Ur, Phys. Rev. C **52**, R6 (1995).
[10] C. M. Petrache *et al.*, Phys. Rev. Lett. **77**, 239 (1996).
[11] C. M. Petrache *et al.*, Phys. Lett. B **415**, 223 (1997).
[12] M. Meyer and J. P. Vivien, Ann. Phys. (Paris) **17**, 11 (1992).
[13] B. J. P. Gall *et al.*, Phys. Lett. B **345**, 124 (1995).
[14] D. Ye *et al.*, Phys. Rev. C **41**, R13 (1990).
[15] M. A. Riley *et al.*, Nucl. Phys. **A512**, 178 (1990).
[16] W. Satuła and R. Wyss, Phys. Rev. C **50**, 2888 (1994).
[17] S. Bouneau *et al.*, Phys. Rev. C **53**, R9 (1996).
[18] C. M. Petrache *et al.*, Phys. Lett. B **373**, 275 (1996).
[19] J. Simpson, Z. Phys. A **358**, 139 (1997).
[20] C. M. Petrache *et al.*, Phys. Lett. B **383**, 145 (1996).
[21] I. Deloncle, M. G. Porquet, and M. Dziri-Marce, Nucl. Instrum. Methods Phys. Res. A **357**, 150 (1995).
[22] C. Beausang *et al.*, Nucl. Instrum. Methods Phys. Res. A **364**, 560 (1996).
[23] K. S. Krane, Nucl. Data Tables **11**, 407 (1973).
[24] C. M. Petrache *et al.*, Phys. Rev. C **53**, R2581 (1996).
[25] R. M. Clark *et al.*, Phys. Lett. B **343**, 59 (1995).
[26] R. B. Firestone, in *Table of Isotopes*, 8th ed., edited by V.S. Shirley (Wiley, New York, 1996).
[27] N. Redon, J. Meyer, Ph. Quentin, P. Bonche, H. Flocard, and P. H. Heenen, Phys. Rev. C **38**, 550 (1988); N. Redon, Ph.D. thesis, Lyon-1 University, 1987.
[28] W. Nazarewicz, R. Wyss, and A. Johnson, Nucl. Phys. **A503**, 285 (1989).
[29] G. de Angelis, Phys. Rev. C **53**, 679 (1996).
[30] R. Wyss *et al.*, Nucl. Phys. **A505**, 337 (1989).
[31] C. M. Petrache *et al.*, Proceedings of the International Conference on Nuclear Structure '98, Gatlinburg, Tennessee 1998, edited by C. Backtash (in press).
[32] T. L. Khoo *et al.*, Phys. Rev. Lett. **76**, 1583 (1996).
[33] G. Hackman *et al.*, Phys. Rev. Lett. **79**, 4100 (1997).
[34] M. J. Brinkman *et al.*, Phys. Rev. C **53**, 1461 (1996).
[35] A. Lopez-Martens *et al.*, Phys. Lett. B **380**, 18 (1996).
[36] K. Hauschild *et al.*, Phys. Rev. C **55**, 2819 (1997).
[37] T. Døssing *et al.*, Phys. Rev. Lett. **75**, 1276 (1995).
[38] D. Madland and J. Nix, Nucl. Phys. **A476**, 1 (1988).
[39] P. Ring and P. Schuck, *The Nuclear Many Body Problem* (Springer-Verlag, New York, 1980).
[40] A. Bohr and B. R. Mottelson, *Nuclear Structure*, Vol. II (World Scientific, Singapore, 1998).
[41] W. Satuła, J. Dobaczewski, and W. Nazarewicz, Phys. Rev. Lett. **81**, 3599 (1998).
[42] D. P. McNabb *et al.*, Phys. Rev. C **56**, 2474 (1997).
[43] S. Perries *et al.*, Z. Phys. A **356**, 1 (1996).
[44] M. Meyer *et al.* (unpublished).
[45] K. Jain *et al.*, Phys. Lett. B **322**, 27 (1994).
[46] K. Tanabe and K. Sugawara-Tanabe, Phys. Lett. B **259**, 12 (1991).